

# Alagebrium Reduces Glomerular Fibrogenesis and Inflammation Beyond Preventing RAGE Activation in Diabetic Apolipoprotein E Knockout Mice

Anna M.D. Watson,<sup>1</sup> Stephen P. Gray,<sup>1</sup> Li Jiaze,<sup>1,2</sup> Aino Soro-Paavonen,<sup>3</sup> Benedict Wong,<sup>1</sup> Mark E. Cooper,<sup>1,2</sup> Angelika Bierhaus,<sup>4</sup> Raelene Pickering,<sup>1</sup> Christos Tikellis,<sup>1</sup> Despina Tsorotes,<sup>1</sup> Merlin C. Thomas,<sup>1,2</sup> and Karin A.M. Jandeleit-Dahm<sup>1,2</sup>

Advanced glycation end products (AGEs) are important mediators of diabetic nephropathy that act through the receptor for AGEs (RAGE), as well as other mechanisms, to promote renal inflammation and glomerulosclerosis. The relative contribution of RAGE-dependent and RAGE-independent signaling pathways has not been previously studied in vivo. In this study, diabetic *RAGE apoE* double-knockout (KO) mice with streptozotocin-induced diabetes were treated with the AGE inhibitor, alagebrium (1 mg/kg/day), or the ACE inhibitor, quinapril (30 mg/kg/day), for 20 weeks, and renal parameters were assessed. RAGE deletion attenuated mesangial expansion, glomerular matrix accumulation, and renal oxidative stress associated with 20 weeks of diabetes. By contrast, inflammation and AGE accumulation associated with diabetes was not prevented. However, treatment with alagebrium in diabetic *RAGE apoE* KO mice reduced renal AGE levels and further reduced glomerular matrix accumulation. In addition, even in the absence of RAGE expression, alagebrium attenuated cortical inflammation, as denoted by the reduced expression of monocyte chemoattractant protein-1, intracellular adhesion molecule-1, and the macrophage marker cluster of differentiation molecule 11b. These novel findings confirm the presence of important RAGE-independent as well as RAGE-dependent signaling pathways that may be activated in the kidney by AGEs. This has important implications for the design of optimal therapeutic strategies for the prevention of diabetic nephropathy. *Diabetes* 61:2105–2113, 2012

**P**rolonged hyperglycemia, dyslipidemia, and oxidative stress in diabetes result in the accumulation of advanced glycation end products (AGEs), which contribute to the development and progression of renal damage (1,2) as well as other diabetes complications (3). The importance of AGEs as downstream mediators of renal damage has been demonstrated in studies using chemically disparate inhibitors of AGE formation to retard the development of kidney disease, including aminoguanidine (4), pyridoxamine (5), benfotiamine (6), and alagebrium chloride (4,7). Furthermore, direct

exposure to AGEs is able to generate lesions similar to those seen in diabetic nephropathy (8). AGEs partly act through receptor-dependent mechanisms to promote vascular damage, cellular dysfunction, fibrogenesis, and inflammation associated with diabetic nephropathy (9,10). The best studied is activation of the receptor for AGEs (RAGE). Genetic deletion of RAGE results in reduced renal injury associated with diabetes (11,12), whereas mice overexpressing RAGE develop severe nephropathy after the induction of diabetes (13). Treatment of diabetic *db/db* mice with soluble RAGE, a dummy receptor that acts as a competitive antagonist to full length RAGE, also significantly reduces renal injury in experimental diabetes (14). Whether the renoprotective actions of AGE inhibitors, such as alagebrium, are predominantly due to their ability to reduce activation of the RAGE receptor associated with a fall in AGE ligands, attenuation of receptor-independent effects of AGEs on kidney function, or both, is unclear. To address this question, in this study, we examine for the first time the renoprotective actions of alagebrium in diabetic *RAGE apoE* double-knockout (KO) mice, with a particular emphasis on glomerular fibrosis and inflammation, comparing its effects with those of the ACE inhibitor, quinapril.

## RESEARCH DESIGN AND METHODS

**Animals.** The effect of diabetes on renal damage and dysfunction was studied in male *apoE* KO mice backcrossed 20 times onto a C57Bl6 background. Diabetes was induced at age 6 weeks by five daily injections of streptozotocin (55 mg/kg; Sigma-Aldrich, St. Louis, MO) in citrate buffer ( $n = 20/\text{group}$ ), with control mice receiving citrate alone. This is a model of accelerated renal damage associated with diabetes, with a more advanced phenotype observed than in wild-type C57Bl6 mice, due to the presence of dyslipidemia, which is also a feature of diabetic nephropathy in humans. All animals were housed at the Precinct Animal Centre, Baker IDI Heart and Diabetes Research Institute. The animals had unrestricted access to water and food and were maintained on a 12-h light–12-h dark cycle on standard mouse chow (Specialty Feeds, Glen Forrest, WA, Australia). Studies were conducted according to National Health and Medical Research Council (NHMRC) guidelines in line with international standards approved by the precinct animal ethics committee.

To examine the effect of RAGE in this model, *apoE* KO mice and *RAGE apoE* double-KO mice on the same C57Bl6 background were studied, as previously described (15). *RAGE apoE* mice were further randomized to be treated with alagebrium (1 mg/kg/day by gavage; Synvista, Ramsay, NY), quinapril (30 mg/kg/day in drinking water; Pfizer, Ann Arbor, MI), or no treatment ( $n = 20/\text{group}$ ). After 20 weeks of diabetes, mice were placed into individual metabolic cages for 24 h and urine was collected. Body weight as well as fluid and food intake were recorded. Urinary albumin excretion was estimated in urine samples by a mouse albumin enzyme-linked immunosorbent assay (ELISA) kit (Bethyl Laboratories, Montgomery, TX) according to the kit protocol. Urinary and serum creatinine concentrations were measured by high-performance liquid chromatography (HPLC) as described previously (16). Systolic blood pressure was assessed by a noninvasive tail cuff method (model ML125, AD Instruments, Bella Vista, NSW, Australia) in conscious mice at the end of the study, as described previously (17).

From the <sup>1</sup>Diabetes Complications Division, Diabetes and Kidney Disease, Baker IDI Heart and Diabetes Research Institute, Melbourne, Victoria, Australia; the <sup>2</sup>Department of Medicine, Monash University, Melbourne, Victoria, Australia; the <sup>3</sup>Division of Nephrology, Department of Medicine, Helsinki University Central Hospital, Helsinki, Finland; and the <sup>4</sup>Department of Medicine, University of Heidelberg, Heidelberg, Germany.

Corresponding author: Anna M.D. Watson, [anna.watson@bakeridi.edu.au](mailto:anna.watson@bakeridi.edu.au).

Received 6 November 2011 and accepted 10 March 2012.

DOI: 10.2337/db11-1546

This article contains Supplementary Data online at <http://diabetes.diabetesjournals.org/lookup/suppl/doi:10.2337/db11-1546/-/DC1>.

© 2012 by the American Diabetes Association. Readers may use this article as long as the work is properly cited, the use is educational and not for profit, and the work is not altered. See <http://creativecommons.org/licenses/by-nc-nd/3.0/> for details.

Mice were humanely killed using a lethal injection of sodium pentobarbitone (100 mg/kg body weight; Euthal, Sigma-Aldrich, Castle Hill, NSW, Australia), followed by cardiac exsanguination. Lysates of erythrocytes were analyzed for glycated hemoglobin levels by HPLC (Bio-Rad, Richmond, CA) (18). Plasma levels of total cholesterol and triglycerides were measured with a standard commercial enzymatic assay using a Beckman Coulter LX20PRO Analyzer (Cat No. 467825 Beckman Coulter Diagnostics, Gladesville, NSW, Australia). LDL cholesterol was calculated using the Friedewald formula. Kidneys were rapidly dissected and weighed (wet weight) before both organs were snap frozen in liquid nitrogen and stored at  $-80^{\circ}\text{C}$  or put in 10% buffered formalin (v/v) before being embedded in paraffin.

**Quantitative real-time RT-PCR.** Glomeruli were isolated from frozen cortical tissue sections by differential sieving. Briefly, frozen cortex was minced on ice using a scalpel blade. The minced cortex was flushed through a 100- $\mu\text{m}$  disposable filter (BD Bioscience, North Ryde, NSW, Australia) with cold saline and collected. The filtered solution was then flushed through a 70- $\mu\text{m}$  filter (BD Bioscience). The glomerular fraction was isolated by inversion of the 70- $\mu\text{m}$  filter, followed by a cold saline flush. The presence of glomeruli was confirmed by light microscopy. The glomerular fraction was then spun at 6,000 rpm for 15 min at  $4^{\circ}\text{C}$ . The supernatant was removed, and the pellets were resuspended in Trizol (1 mL). RNA isolation and cDNA generation were done as described previously (16). Gene expression of key matrix proteins, adhesion molecules, and proinflammatory cytokines were assessed by real-time quantitative RT-PCR using the Taqman system based on the real-time detection of accumulated fluorescence (ABI Prism 7500; Perkin-Elmer, Foster City, CA; see the Supplementary Table for probes and primers) (16). Gene expression was normalized to 18S mRNA and reported as ratios compared with the level of expression in untreated control mice, which were given an arbitrary value of 1.

**Histochemistry on renal sections.** Kidney sections (2  $\mu\text{m}$ ) were stained with periodic acid-Schiff (PAS) for measurement of mesangial area. Mesangial area was analyzed (percentage of glomerular area) from digital pictures of glomeruli (15–20 glomeruli per kidney per animal) using Image-Pro Plus 6.0 software (Media Cybernetics, Bethesda, MD), as described previously (16). Sections were also stained for collagen IV antibody (1:1600 goat anti-collagen IV, Southern Biotech, Birmingham, AL), fibronectin (1:100 rabbit anti-fibronectin, Dako Cytomation, Glostrup, Denmark), monocyte chemoattractant protein (MCP)-1 (1:50 hamster anti-macrophage chemoattractant protein-1 BD Pharmingen, North Ryde, NSW, Australia), AGEs (antibody kindly provided by M. Coughlan, Baker IDI Heart and Diabetes Institute, Melbourne, VIC, Australia (19)), and nitrotyrosine (1:200 rabbit anti-nitrotyrosine, Millipore, Australia). For glomerular assessment,  $\sim 15$  glomeruli/slide were captured as photomicrographs (Olympus BX-50, Olympus Optical; Q-imaging MicroPublisher 3.3 RTV camera, Surrey, BC, Canada) under identical light conditions, and the percentage of the area of the glomerular tuft stained was digitally quantitated based on red, green, and blue (Image Pro-Plus 6.0 software; Media Cybernetics, Silver Spring, MD). The tubulointerstitial area was assessed using a point-based system, as described previously (20), with six fields (magnification  $\times 200$ ) assessed per animal ( $n = 6$ –8 per group).

**Protein quantification.** Protein extracts from kidney cortex for each group ( $n = 5$ –6/group) were used to estimate the concentration the expression of intracellular adhesion molecule (ICAM)-1 and MCP-1 (both R&D Systems, Bio Scientific, Kirrawee, NSW, Australia) according to ELISA kit instructions, except homogenate for MCP-1 was used at 1:2. AGEs were determined using a direct ELISA, as previously described (21), using the antibody described above used for immunohistochemistry. Cluster of differentiation molecule 11b (CD11b), which is part of macrophage-1 (Mac-1) antigen, was determined using a sandwich ELISA. High-binding 96-well ELISA plates were coated overnight at  $4^{\circ}\text{C}$  in  $1\times\text{PBS}$  with mouse anti-CD11b (ED8, Novus Biologicals, Sapphire Bioscience, Waterloo, NSW, Australia). After all steps, three washes with  $1\times\text{PBS}/0.05\%$  Tween 20 (PBS/T) were performed. Plates were blocked with 4% milk/PBS/T for 2 h at room temperature (RT) before mouse kidney homogenates were added (1:2; 2 h RT). Rat anti-CD11b monoclonal antibody (M1/70, eBioscience, Jomar Bioscience Kensington, SA, Australia) was then added (2 h, 1:500 in 0.4% milk/PBS/T), followed by detection with biotinylated anti-rat IgG (1 h, RT), streptavidin horseradish peroxidase (R&D Systems) for 30 min at RT, then 100  $\mu\text{L}$ /well of 3,3',5,5'-tetramethylbenzidine (TMB) liquid substrate (Sigma). The optical density was scanned at 655 nm. BCA protein assay (Pierce, Thermo Scientific, Scoresby, VIC, Australia) was performed (samples 1:40 in PBS) according to kit instructions, and ELISA results were expressed relative to the total protein concentration.

**Statistical analysis.** Data were analyzed by one-way ANOVA with comparisons of group means performed by the Fisher least significant difference method. Analyses were performed using SPSS 17.0 software (SPSS, Chicago, IL). Data are shown as means  $\pm$  SEM unless otherwise specified; albuminuria is shown as the geometric mean.  $P < 0.05$  was considered statistically significant.

## RESULTS

**Metabolic parameters.** The induction of diabetes was associated with elevated plasma glucose concentrations and glycated hemoglobin levels compared with the respective nondiabetic controls, which were comparable in *apoE* KO and *RAGE apoE* double-KO mice (Table 1). Glucose and glycated hemoglobin were not significantly affected by treatment with alagebrium or quinapril in diabetic mice. Total and LDL cholesterol were also higher in diabetic mice compared with nondiabetic controls. Diabetes in *RAGE apoE* KO mice was associated with modestly lower total and LDL cholesterol levels, although plasma levels remained markedly elevated due to the deficiency of the *apoE* gene. Lipid parameters were not significantly modified in mice treated with alagebrium or quinapril. Systolic blood pressure levels did not significantly differ between *apoE* KO and *RAGE apoE* double-KO mice or with

TABLE 1

General and metabolic parameters after 20 weeks of study in *apoE* KO and *RAGE apoE* double-KO mice, in the presence and absence of diabetes, with and without treatment ( $n = 8$ –11 per group)

	Control		Diabetes			
	<i>ApoE</i> KO	<i>RAGE apoE</i>	<i>ApoE</i> KO	<i>RAGE apoE</i> KO	<i>RAGE apoE</i> KO +	
					Quinapril	Alagebrium
Systolic blood pressure (mmHg)	124 $\pm$ 2	117 $\pm$ 6	127 $\pm$ 4	126 $\pm$ 6	103 $\pm$ 4#§	130 $\pm$ 4
Body weight (g)	31.8 $\pm$ 0.5	37.6 $\pm$ 1.0*	23.8 $\pm$ 0.4*	26.6 $\pm$ 1.0§¶	28.1 $\pm$ 0.5§	28.3 $\pm$ 0.9§
Kidney weight (g/mm <sup>2</sup> )	35.6 $\pm$ 0.7	35.1 $\pm$ 1.0	50.2 $\pm$ 1.0*	47.9 $\pm$ 1.2¶	48.0 $\pm$ 1.1	45.1 $\pm$ 1.5§
Albumin excretion ( $\mu\text{g}/24$ h)	26	38	160*	186¶	115#	156
Creatinine clearance (mL/min/m <sup>2</sup> )	42 $\pm$ 5	33 $\pm$ 4	66 $\pm$ 8*	73 $\pm$ 4¶	67 $\pm$ 6	54 $\pm$ 2†
Glycated hemoglobin (%)	4.3 $\pm$ 0.1	4.1 $\pm$ 0.2	14.3 $\pm$ 0.4*	13.7 $\pm$ 0.5¶	13.8 $\pm$ 0.3	13.8 $\pm$ 0.4
Plasma glucose (mmol/L)	10.5 $\pm$ 0.7	12.6 $\pm$ 0.6	35.0 $\pm$ 2.0*	33.0 $\pm$ 1.9¶	32.1 $\pm$ 2.6	29.5 $\pm$ 2.3§
Total cholesterol (mmol/L)	10.5 $\pm$ 2.7	11.4 $\pm$ 0.5	21.2 $\pm$ 1.2*	16.9 $\pm$ 1.2§¶	18.3 $\pm$ 1.8	16.2 $\pm$ 1.1§
Triglycerides (mmol/L)	1.5 $\pm$ 0.1	2.2 $\pm$ 0.4	2.1 $\pm$ 0.3	1.5 $\pm$ 0.3	2.3 $\pm$ 0.3	1.6 $\pm$ 0.2
HDL (mmol/L)	2.4 $\pm$ 0.2	2.9 $\pm$ 0.1	3.8 $\pm$ 0.2*	3.2 $\pm$ 0.2	3.6 $\pm$ 0.4	2.9 $\pm$ 0.7‡§
LDL (mmol/L)	7.3 $\pm$ 0.5	7.5 $\pm$ 0.4	16.5 $\pm$ 1.0*	13.1 $\pm$ 0.9§¶	13.7 $\pm$ 1.3§	12.6 $\pm$ 1.0§

Albumin excretion is expressed as the geometric mean. \* $P < 0.05$  vs. *ApoE* KO. § $P < 0.05$  vs. diabetic *apoE* KO. ¶ $P < 0.05$  vs. *RAGE apoE* KO. # $P < 0.05$  diabetic *RAGE apoE* KO vs. diabetic *RAGE apoE* KO + quinapril. † $P < 0.05$  diabetic *RAGE apoE* KO vs. diabetic *RAGE apoE* + alagebrium. ‡ $P < 0.05$  diabetic *RAGE apoE* KO + quinapril vs. diabetic *RAGE apoE* KO + alagebrium.

the induction of diabetes. Blood pressure was reduced in mice treated with the ACE inhibitor, quinapril, but was not affected by treatment with alagebrium (Table 1).

**Renal function, albuminuria, and renal hypertrophy.** The induction of diabetes was associated with increased 24-h urinary albumin excretion compared with nondiabetic *apoE* KO mice (Table 1). Neither RAGE deletion nor alagebrium treatment reduced albuminuria in this model (Table 1). However, treatment with quinapril significantly lowered albumin excretion by 30% in diabetic *RAGE apoE* double-KO mice (Table 1). After 20 weeks of diabetes, kidney weight and creatinine clearance were increased in diabetic mice, with similar changes observed in *apoE* KO and *RAGE apoE* double-KO mice compared with their respective nondiabetic controls (Table 1). In diabetic *RAGE apoE* double-KO mice, treatment with alagebrium was associated with a modest reduction in renal mass and reduced hyperfiltration compared with nontreated mice, whereas treatment with quinapril had no effect (Table 1).

**Mesangial area.** Mesangial area was assessed on PAS-stained sections (Fig. 1) and expressed as a percentage of glomerular area (Fig. 1G). After 20 weeks of diabetes, the mesangial area was significantly increased in diabetic *apoE* KO mice compared with nondiabetic *apoE* KO mice (Fig. 1). Mesangial expansion associated with the induction of diabetes in *RAGE apoE* double-KO mice was reduced. This decrease in mesangial area was not further attenuated by treatment with alagebrium or quinapril. Neither alagebrium nor quinapril treatment affected mesangial area in nondiabetic *RAGE apoE* double-KO mice (data not shown).

**Glomerular fibrosis and inflammation.** Glomerular matrix accumulation is the hallmark of diabetic kidney disease. The expression of collagen IV in glomeruli was significantly increased in diabetic *apoE* KO mice at a gene (Table 2) and protein level (Fig. 2). *RAGE* deletion was associated with a reduction in glomerular collagen IV expression in diabetic *RAGE apoE* double-KO mice. Treatment with alagebrium or quinapril in diabetic *RAGE apoE* double-KO mice was associated with a further reduction in glomerular collagen IV levels, approaching levels observed in control mice (Fig. 2g). The expression of fibronectin was also increased in glomeruli from diabetic *apoE* KO mice at the gene (diabetic,  $2.6 \pm 0.4$ -fold induction; control,  $1.0 \pm 0.1$ -fold induction;  $P < 0.01$ ) and protein level (Fig. 2n). *RAGE* deletion was also associated with a reduction in fibronectin protein in the glomeruli of diabetic *RAGE apoE* KO mice (Fig. 2n). Treatment with alagebrium and quinapril further reduced fibronectin protein accumulation in the glomeruli from diabetic *RAGE apoE* double-KO mice (Fig. 2n). There was no significant increase in the tubulointerstitial area after 20 weeks of diabetes compared with nondiabetic controls. The cortical (tubular) expression of collagen IV and fibronectin were also not changed by diabetes (data not shown).

Diabetes was also associated with the induction of gene expression of key fibrogenic growth factors in the glomeruli, including mRNA-encoding transforming growth factor- $\beta$  (*tgfb1*), connective tissue growth factor (*ctgf*), vascular endothelial growth factor (*vegfa*), and the p65 subunit of nuclear factor- $\kappa$ B (NF- $\kappa$ B; *rela*; Table 2). *RAGE* deletion attenuated induction of *ctgf*, *vegfa*, and *rela* associated with diabetes. However, the glomerular gene expression of *tgfb1* (encoding TGF- $\beta$ ) was unaffected. Treatment with alagebrium and quinapril in *RAGE apoE* double-KO mice did not further reduce gene expression beyond that observed in *RAGE apoE* double-KO mice.

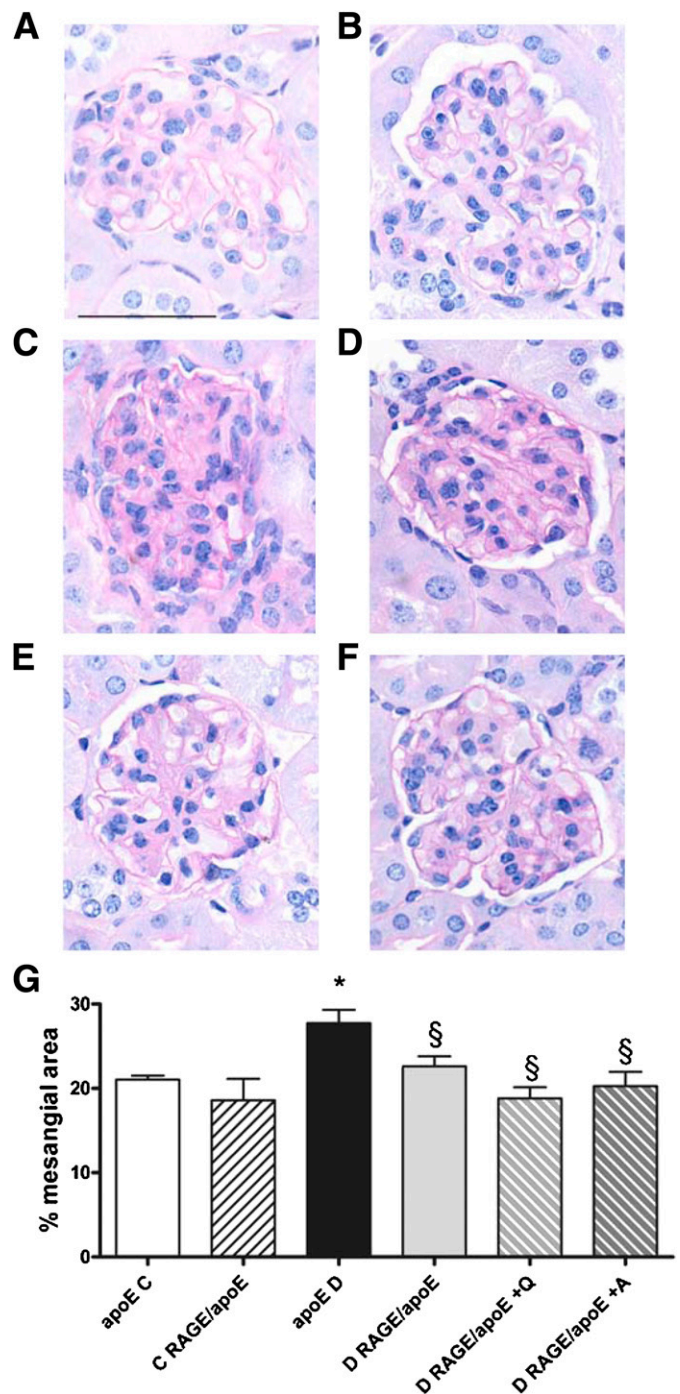


FIG. 1. PAS staining in control (C) and diabetic (D) *apoE* KO and *RAGE apoE* double-KO mice, with and without treatment: *apoE* KO (A); *RAGE apoE* KO (B); diabetic *apoE* KO (C); diabetic *RAGE apoE* KO (D); *RAGE apoE* KO + alagebrium (A) 1 mg/kg/day (E); and diabetic *RAGE apoE* KO + quinapril (Q) 30 mg/kg/day (F). Scale bar in A = 100  $\mu$ m. Digital quantification of mesangial area (G) for  $n = 6-8$  per group. \* $P < 0.05$  vs. *apoE* KO. § $P < 0.05$  vs. diabetic *apoE* KO. (A high-quality color representation of this figure is available in the online issue.)

**Glomerular inflammation.** Diabetes is associated with the recruitment and retention of macrophages in glomeruli, as indicated by increased expression of the macrophage marker CD11b at the gene and protein level (Fig. 3) and its cognate receptor, the adhesion molecule ICAM-1 (Fig. 3). Expression of the chemokine MCP-1 was also increased

TABLE 2

Analysis of mRNA expression in isolated renal glomeruli from *apoE* KO and *RAGE apoE* double-KO mice, in the presence and absence of diabetes, with and without treatment ( $n = 5-8$  per group)

	Control		Diabetes			
	<i>ApoE</i> KO	<i>RAGE apoE</i> KO	<i>ApoE</i> KO	<i>RAGE apoE</i> KO	<i>RAGE apoE</i> KO +	
					Quinapril	Alagebrium
<i>ager</i> (RAGE)	1.0 ± 0.2	—	2.1 ± 0.3*	—	—	—
<i>ddost</i> (AGE-R1)	1.0 ± 0.1	1.9 ± 0.3*	1.2 ± 0.1	1.6 ± 0.2	1.3 ± 0.1	1.3 ± 0.1
<i>prkcsh</i> (AGE-R2)	1.0 ± 0.1	1.2 ± 0.2	1.1 ± 0.1	0.9 ± 0.1	0.5 ± 0.0#§	0.7 ± 0.1§
<i>lgals3</i> (AGE-R3)	1.0 ± 0.1	1.7 ± 0.2*	2.1 ± 0.1*	1.6 ± 0.1§	1.6 ± 0.2§	1.3 ± 0.1§
<i>col4a1</i> (collagen IV)	1.0 ± 0.2	1.4 ± 0.2	2.1 ± 0.4*	1.4 ± 0.1§	1.2 ± 0.1§	1.1 ± 0.1§
<i>tgfb1</i> (TGF-β)	1.0 ± 0.1	1.6 ± 0.2*	1.8 ± 0.2*	1.7 ± 0.2	2.0 ± 0.1	1.4 ± 0.1‡
<i>ctgf</i> (CTGF)	1.0 ± 0.1	1.5 ± 0.1	2.9 ± 0.5*	1.6 ± 0.3§	2.6 ± 0.1#	1.8 ± 0.1§‡
<i>vegfa</i> (VEGF)	1.0 ± 0.1	1.0 ± 0.1	1.6 ± 0.3*	1.1 ± 0.1§	0.9 ± 0.1§	0.8 ± 0.0§
<i>rela</i> (NFκB p65)	1.0 ± 0.1	1.7 ± 0.2*	2.0 ± 0.3*	1.2 ± 0.1§¶	1.4 ± 0.1§	1.1 ± 0.0§

Student *t* test was used for the *ager* (RAGE) comparison. Encoding proteins are in parentheses. \* $P < 0.05$  vs. *apoE* control. § $P < 0.05$  vs. *apoE* diabetic. ¶ $P < 0.05$  vs. *RAGE apoE* control. # $P < 0.05$  *RAGE apoE* diabetic vs. *RAGE apoE* diabetic + quinapril. ‡ $P < 0.05$  *RAGE apoE* diabetic + quinapril vs. *RAGE apoE* diabetic and alagebrium.

in the diabetic kidney (Fig. 4). The expression of CD11b, ICAM-1, and MCP-1 associated with diabetes was not attenuated in diabetic *RAGE apoE* double-KO mice. However, treatment with alagebrium and quinapril were able to significantly reduce the expression of these inflammatory mediators and markers in the absence of RAGE (Figs. 3 and 4).

**Oxidative stress.** Oxidative stress is a key mediator of renal injury in the diabetic kidney. After 20 weeks of diabetes, nitrotyrosine staining, a marker of oxidative damage, was increased in the glomeruli of diabetic *apoE* KO mice (Fig. 5). Nitrotyrosine staining was reduced in diabetic *apoE RAGE* double-KO mice. There was trend for a further reduction in nitrotyrosine staining with quinapril ( $P = 0.08$ ) and alagebrium in diabetic *apoE RAGE* double-KO mice, but these changes did not reach statistical significance (Fig. 5).

**Total tissue AGE and RAGEs.** Diabetes was associated with an increase in the AGE content in renal cortex as assessed by ELISA (Fig. 6). RAGE deficiency was not associated with any reduction in renal AGE accumulation in diabetic mice (Fig. 6). However, treatment with alagebrium or quinapril were both associated with a reduction in total renal AGE content and glomerular AGE staining, consistent with their known effects on inhibiting AGE generation (19,22,23). Diabetes was also associated with an eightfold increase in the expression of RAGE mRNA (*ager*) in cortical extracts. In addition, the expression of *lgals3* (encoding AGE-R3) was also increased after 20 weeks of diabetes, whereas *ddost* (encoding AGE-R1) and *prkcsh* (encoding AGE-R2) were unaltered (Table 2). These changes associated with diabetes were not significantly affected by RAGE deletion, although RAGE deletion itself was associated with a modest increase in the gene expression of *ddost* (encoding AGE-R1) and *prkcsh* (encoding AGE-R3) nondiabetic *apoE* KO mice. Treatment with alagebrium or quinapril reduced the expression of each of these RAGEs in *RAGE apoE* double-KO mice, as previously reported (24).

## DISCUSSION

Inhibition of AGE accumulation is renoprotective in experimental diabetes (4). This is partly mediated by reducing

AGE-dependent activation of RAGE and subsequent downstream signaling associated with diabetic nephropathy. Here, for the first time, we demonstrate that the AGE inhibitor, alagebrium chloride, retains some of its renoprotective effects in the diabetic kidney, including reduced glomerular fibrogenesis and attenuated macrophage accumulation, even in the absence of RAGE. By contrast, mesangial expansion was not affected by alagebrium in the absence of RAGE, despite the beneficial effects of alagebrium on mesangial expansion in RAGE-replete mice that we have previously reported in the same model (4). Although similar findings have been suggested by in vitro studies (14,25), our novel data confirm the presence of important RAGE-dependent and RAGE-independent signaling pathways that may be activated in the kidney by AGEs in vivo. These results have important implications for the design of optimal therapeutic strategies for the prevention of diabetic nephropathy.

Our data confirm that attenuation of the AGE-RAGE axis represents at least one mechanism by which AGE inhibition may confer renoprotective benefits. There are strong data to suggest that RAGE signaling is important for the development and progression of diabetic kidney disease. Mice overexpressing RAGE develop severe glomerulosclerosis after the induction of diabetes (13). By contrast, treatment of diabetic *db/db* mice with soluble RAGE (sRAGE), a receptor that acts as a competitive antagonist to full-length RAGE, significantly reduces renal injury in experimental diabetes (14). Similarly, genetic deletion of RAGE in our experiments was associated with reduced mesangial expansion and glomerular injury associated with diabetes in the current study.

In our model, RAGE deletion alone did not reduce diabetes-associated albuminuria, renal hypertrophy, or inflammation associated with diabetes. It is possible to speculate that the modest albuminuria in our model is chiefly hemodynamic and does not accurately reflect renal fibrogenesis because only quinapril reduced diabetes-associated albuminuria, whereas RAGE deletion and alagebrium had clear beneficial effects with respect to fibrogenesis. Discordance between effects on albuminuria and renal fibrosis has been shown previously in studies using other renoprotective agents, including the use of neutralizing

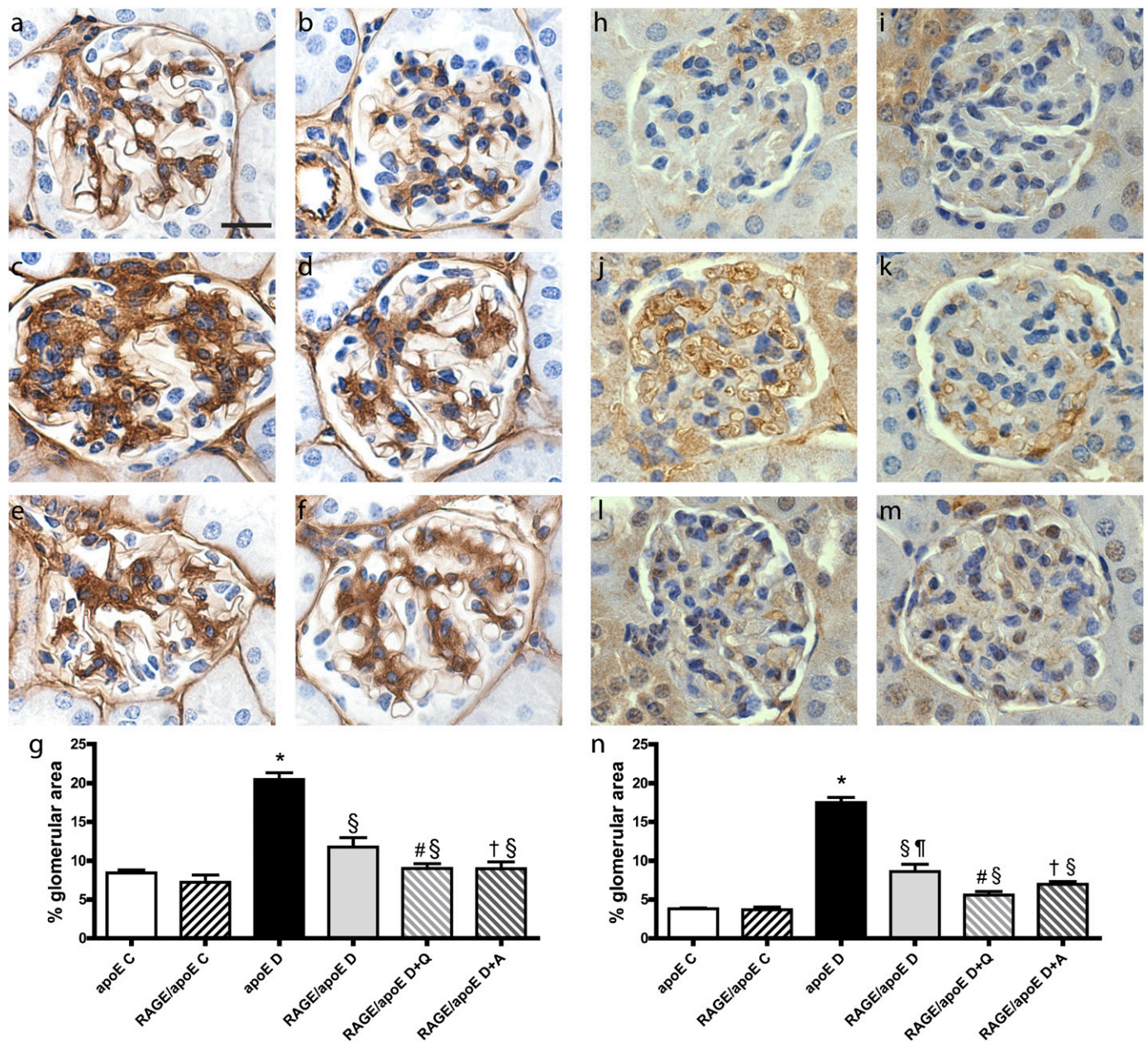


**FIG. 2.** Immunostaining for collagen IV (*a–f*) and fibronectin (*h–m*) in nondiabetic control (C) and diabetic (D) *apoE* KO and *RAGE apoE* double-KO mice, with and without treatment. *apoE* C (*a, h*); *RAGE apoE* KO (*b, i*); *apoE* D (*c, j*); diabetic *RAGE apoE* KO (*d, k*); diabetic *RAGE apoE* KO alagebrum (A) 1 mg/kg/day (*e, l*); diabetic *RAGE/apoE* KO quinapril (Q) 30 mg/kg/day (*f, m*). Scale bar = 20  $\mu$ m. Digital quantification of glomerular staining for collagen IV (*g*) and fibronectin (*n*) for  $n = 6–10$  per group. \* $P < 0.05$  vs. *apoE* KO. § $P < 0.05$  vs. diabetic *apoE*. ¶ $P < 0.05$  vs. *RAGE apoE* KO. # $P < 0.05$  diabetic *RAGE apoE* KO vs. diabetic *RAGE apoE* KO + quinapril. † $P < 0.05$  diabetic *RAGE apoE* KO vs. diabetic *RAGE apoE* KO + alagebrum. (A high-quality color representation of this figure is available in the online issue.)

TGF- $\beta$  antibodies (26). A reduction in diabetes-associated albuminuria in *RAGE* KO mice has been previously reported (12,14). However, the streptozotocin diabetic *apoE* KO mouse used in the current study is characterized by more advanced diabetic lesions than those observed in C57Bl6 and many other mouse models (4). *RAGE* deletion in the OVE26 transgenic diabetic mouse, another relevant model of advanced diabetic nephropathy, is also associated with attenuation of albuminuria (11). However, the OVE model is also associated with increased blood pressure, which is well known to correlate with increased albuminuria (27). *RAGE* deletion in the iNOSTg mouse (CD-1 background) also showed reduced albuminuria, although the effects of *RAGE*

deletion on blood pressure and hemodynamic parameters in that model have not been reported (28).

The ability of AGEs to cause renal damage in the absence of *RAGE* may have several explanations. Firstly, activation of other RAGEs may modify pathogenic pathways in the diabetic kidney, even in *RAGE* KO mice. For example, AGE-R2 is a protein kinase C substrate involved in the p21(ras)–mitogen-activated protein kinase (MAPK) signaling cascade. However, other RAGEs have renoprotective effects. *AGE-R3* receptor KO mice develop accelerated nephropathy after the induction of diabetes (29). In addition, AGE-R1 appears to be a clearance receptor and opposes AGE-mediated mesangial cell inflammation partly

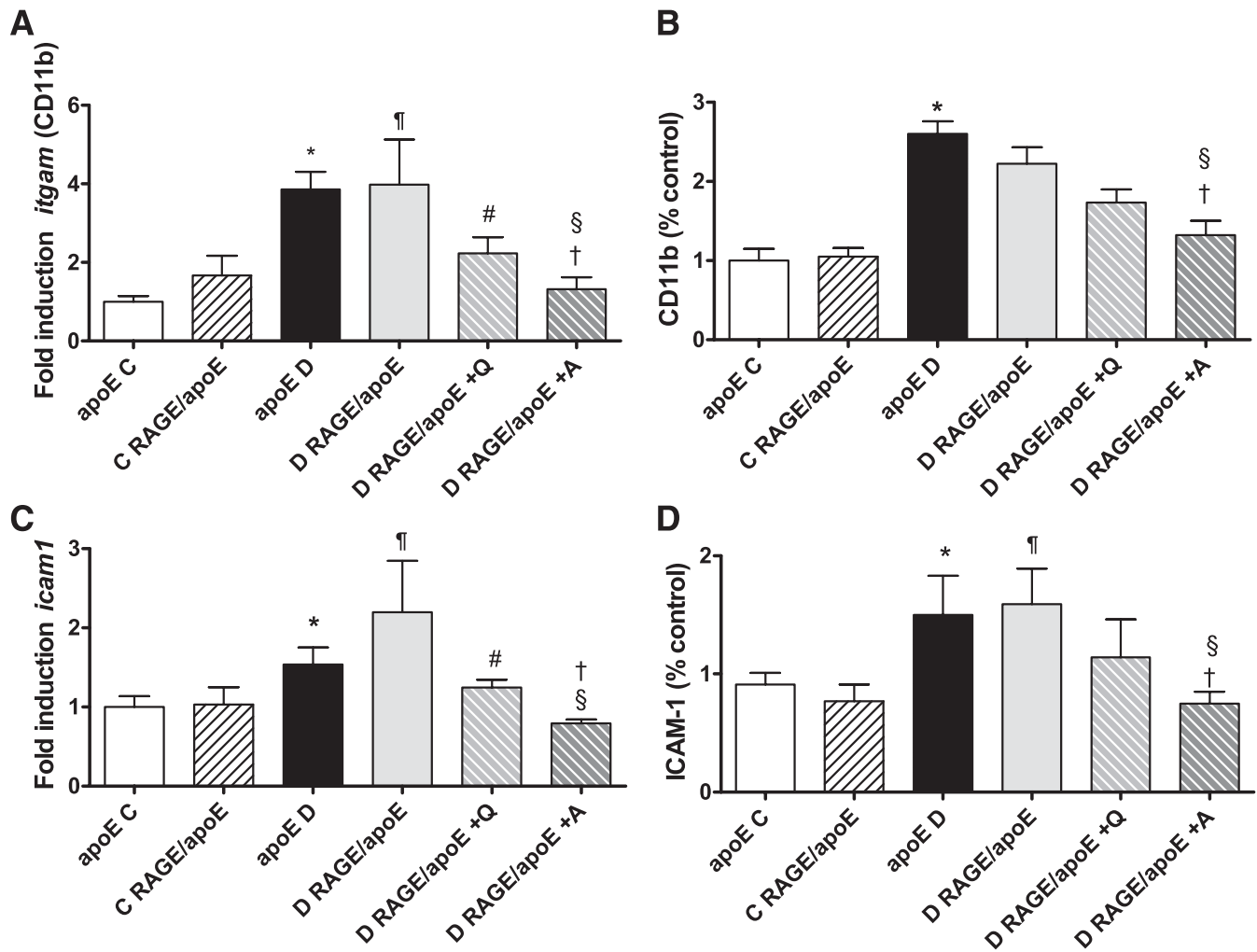


**FIG. 3.** Gene and protein expression of inflammation markers CD11b and ICAM-1 in glomeruli from nondiabetic control (C) and diabetic (D) *apoE* KO and *RAGE apoE* double-KO mice, with and without treatment, as measured by RT-PCR and ELISA. Gene expression of CD11b (A), relative protein content of CD11b (B), gene expression of ICAM-1 (C), and relative protein expression of ICAM-1 (D) for  $n = 6-10$  per group. \* $P < 0.05$  vs. *apoE* KO. § $P < 0.05$  vs. diabetic *apoE*. ¶ $P < 0.05$  vs. *RAGE apoE* KO. # $P < 0.05$  diabetic *RAGE apoE* KO vs. diabetic *RAGE apoE* KO + quinapril. † $P < 0.05$  diabetic *RAGE apoE* KO vs. diabetic *RAGE apoE* KO + alagebrium.

through negative regulation or RAGE signaling (30). Indeed, the gene expression of *ddost* (encoding AGE-R1) and *prkcs* (encoding AGE-R3) were increased in the glomeruli of *RAGE apoE* double-KO mice, potentially contributing the reduced renal injury in these mice. However, RAGE deletion did not alter renal AGE levels in the absence or presence of diabetes, suggesting that AGE-clearance was not enhanced.

Secondly, AGEs may also promote injury directly. Certainly, post-translational modification of amino, guanidino, and thiol functional groups on vulnerable proteins, lipids, and DNA targets has the potential to alter their structure, stability, and/or function (31,32). For example, the AGE-modification of collagen leads to structural alterations, including changes in packing density, self-assembly, and surface charge, as well as heterotypic interactions with laminin and fibronectin (33,34), which potentially contribute to glomerular matrix accumulation and mesangial expansion. AGE modification of antioxidants such as Cu-Zn-superoxide dismutase contributes to the decline in antioxidant activity (35). AGEs can also directly enhance the formation of free radicals through catalytic sites in their molecular structure (36). Indeed, oxidative stress and apoptosis induction by

modified collagen appears to be largely independent of RAGE activation (37).

The current study has specifically focused on early glomerular changes associated with diabetes. Glomerulosclerosis, interstitial fibrosis, or other structural features associated with advanced nephropathy are generally not observed in mice bred on a C57Bl6-background (18). Nonetheless, this model is associated with mesangial expansion, matrix deposition, and macrophage recruitment. In particular, diabetic nephropathy is considered to be an inflammatory disease in which progressive glomerular injury is associated with infiltration by CD11b-positive macrophages (38) mediated by various chemokines secreted from resident glomerular cells, such as MCP-1 (39), and adhesion molecules, such as ICAM-1 (40). In our model, the induction of diabetes was associated with the increase in MCP-1 and ICAM-1 expression in both *apoE* KO and *apoE RAGE* double-KO mice, paralleling the accumulation of macrophages in the cortex, as denoted by the increased expression of the macrophage integrin and leukocyte-adhesion mediator CD11b. Treatment with the AGE inhibitor, alagebrium, reduced expression of MCP-1, ICAM-1, and CD11b, suggesting its anti-inflammatory action is partly independent

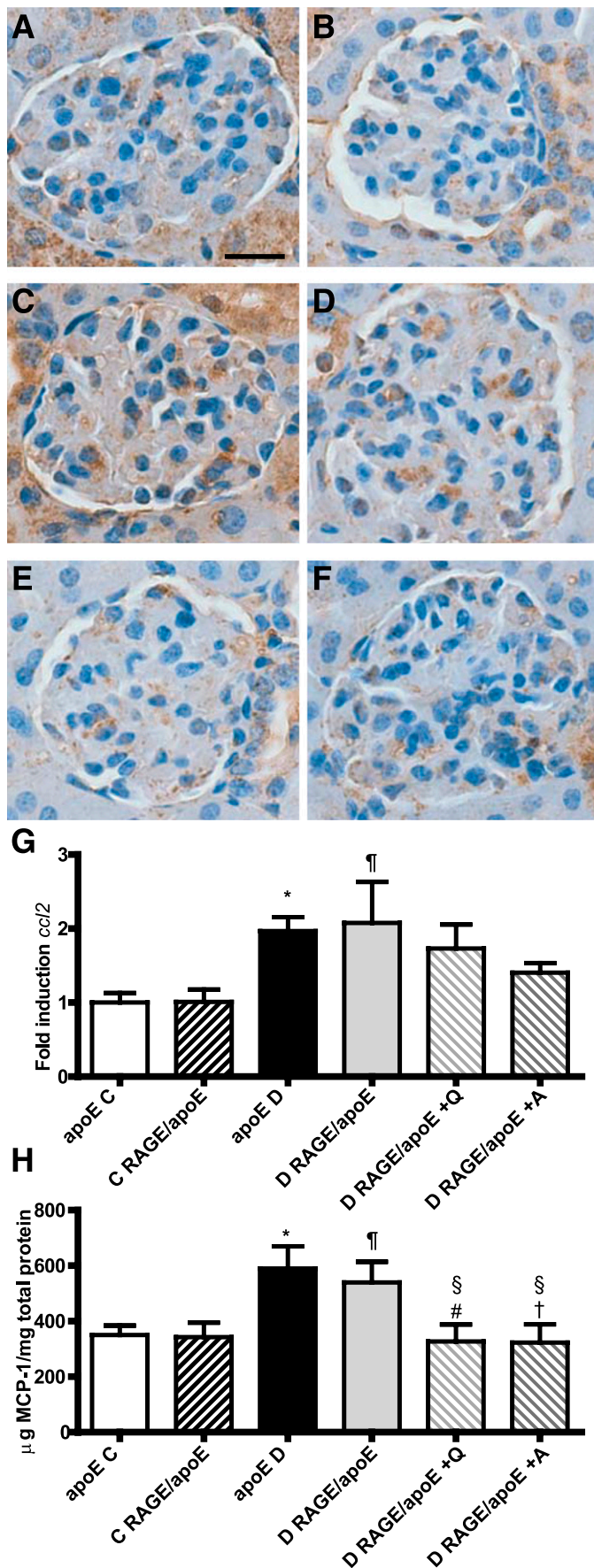


FIG. 4. Immunostaining for MCP-1 in nondiabetic control (C) and diabetic (D) *apoE* KO and *RAGE apoE* double-KO mice, with and without

to the reduction in activation of the RAGE receptor by AGEs. This contrasts with in vitro studies that have suggested that MCP-1 and ICAM-1 are largely RAGE-dependent (30) and may be blocked with neutralizing antibodies to RAGE (41,42). Such differences potentially reflect the use of excessively modified proteins in in vitro systems, which are better (although potentially nonphysiologic) RAGE ligands.

Finally, we have also examined the renoprotective effects of ACE inhibition in the context of RAGE deletion. Previous work has shown that ACE inhibition modifies RAGE signaling (43) and reduces renal AGE content (43,44), which may partly contribute to their beneficial actions in the diabetic kidney. In the current study, however, ACE inhibition with quinapril remained effective in reducing glomerular markers of injury and inflammation associated with diabetes in the absence of RAGE. This is consistent with our previous findings in the spontaneously hypertensive rat where AGE inhibition and blockade of the renin-angiotensin system have synergistic benefits on renal damage associated with diabetes (45).

In summary, our results demonstrate the presence of both RAGE-dependent and RAGE-independent signaling pathways in vivo that may be activated in the diabetic kidney by AGEs. Although *RAGE* deletion partly attenuates the development of diabetes-associated glomerular fibrosis and mesangial expansion in *apoE* KO mice, treatment with the AGE inhibitor, alagebrium, further reduced glomerular fibrosis and attenuated renal inflammation in diabetic *RAGE apoE* double-KO mice. These results suggest that a combination of AGE-lowering therapies and RAGE blockade may have synergistic effects for the prevention of diabetic kidney disease.

#### ACKNOWLEDGMENTS

A.M.D.W. is supported by an NHMRC Australian Biomedical Fellowship (472698). M.E.C. is an NHMRC Australian fellow and recipient of a Juvenile Diabetes Research Foundation (JDRF) Scholars Award. M.C.T. and K.A.M.J.-D. are senior research fellows of the NHMRC of Australia. These studies were supported by grant funding from the NHMRC, JDRF, and the Diabetes Australia Research Trust, and were supported in part by the Victorian Government's Operational Infrastructure Support Program.

No potential conflicts of interest relevant to this article were reported.

A.M.D.W. collected research data, contributed to discussion, and wrote, reviewed, and edited the manuscript. S.P.G. collected research data and reviewed and edited the manuscript. L.J., A.S.-P., B.W., R.P., C.T., and D.T. collected research data and contributed to the manuscript. M.E.C. and A.B. contributed to discussion and wrote and reviewed the manuscript. M.C.T. collected research data and contributed to discussion. K.A.M.J.-D. contributed to

treatment. *ApoE* KO (A); *RAGE/apoE* KO (B); diabetic *apoE* KO (C); diabetic *RAGE apoE* KO (D); diabetic *RAGE apoE* KO + alagebrium (A) 1 mg/kg/day (E); diabetic *RAGE apoE* KO + quinapril (Q) 30 mg/kg/day (F). Renal cortical MCP-1 expression by RT-PCR (G) and ELISA (H) for  $n = 6-8$  per group. Scale bar = 20  $\mu\text{m}$ . \* $P < 0.05$  vs. *apoE* KO. § $P < 0.05$  vs. diabetic *apoE* KO. † $P < 0.05$  vs. *RAGE apoE* KO. # $P < 0.05$  diabetic *RAGE apoE* KO vs. diabetic *RAGE apoE* KO + quinapril. ‡ $P < 0.05$  diabetic *RAGE apoE* KO vs. diabetic *RAGE apoE* KO + alagebrium. (A high-quality digital representation of this figure is available in the online issue.)

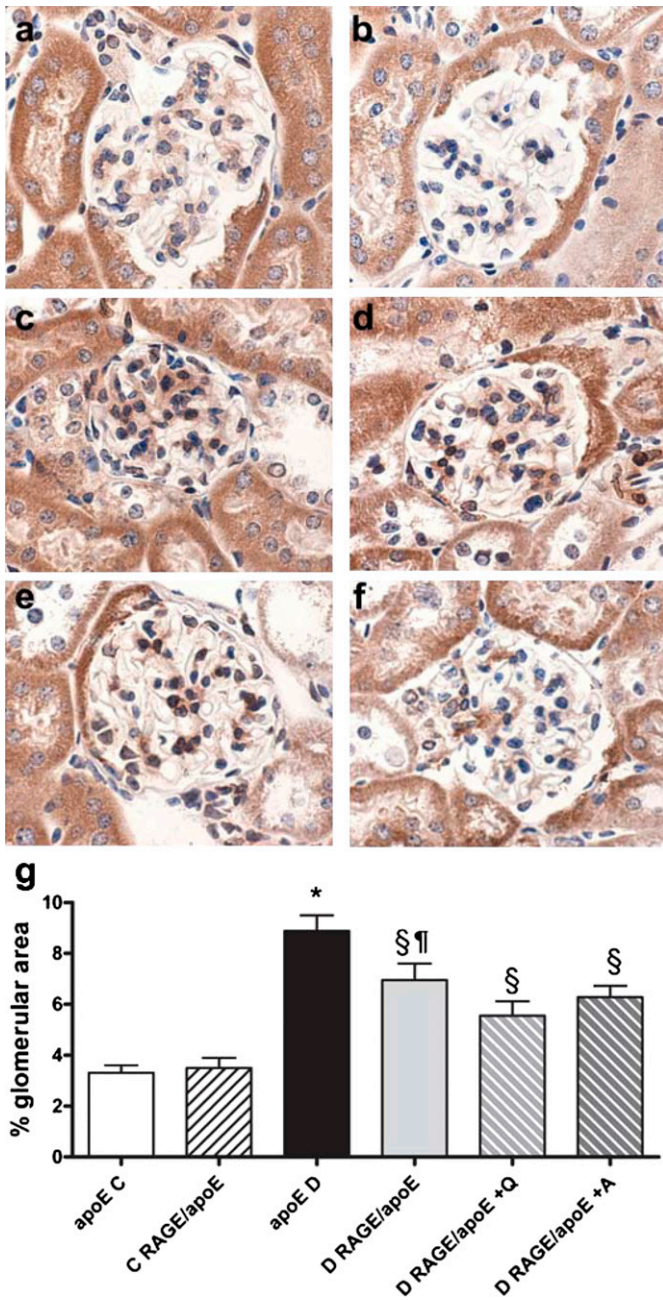


FIG. 5. Immunostaining for the marker of oxidative stress, nitrotyrosine, in nondiabetic control (C) and diabetic (D) *apoE* KO and RAGE *apoE* double-KO mice, with and without treatment. *ApoE* KO (a); RAGE *apoE* KO (b); diabetic *apoE* KO (c); diabetic RAGE *apoE* KO (d); diabetic RAGE *apoE* KO + alagebrium (A) 1 mg/kg/day (e); diabetic RAGE *apoE* KO + quinapril (Q) 30 mg/kg/day (f). Digital quantification (g) for  $n = 6-10$  per group. \* $P < 0.05$  vs. *apoE* KO. § $P < 0.05$  vs. diabetic *apoE* KO. ¶ $P < 0.05$  vs. RAGE *apoE* KO. (A high-quality color representation of this figure is available in the online issue.)

discussion and wrote, reviewed, and edited the manuscript. A.M.D.W. and K.A.M.J.-D. are the guarantors of this work and, as such, had full access to all of the data in the study and take responsibility for the integrity of the data and the accuracy of the data analysis.

The authors thank Dian Samijono for technical assistance and Kylie Gilbert for assistance with the animals (all members of the Baker IDI Heart and Diabetes Institute, Melbourne, Australia).

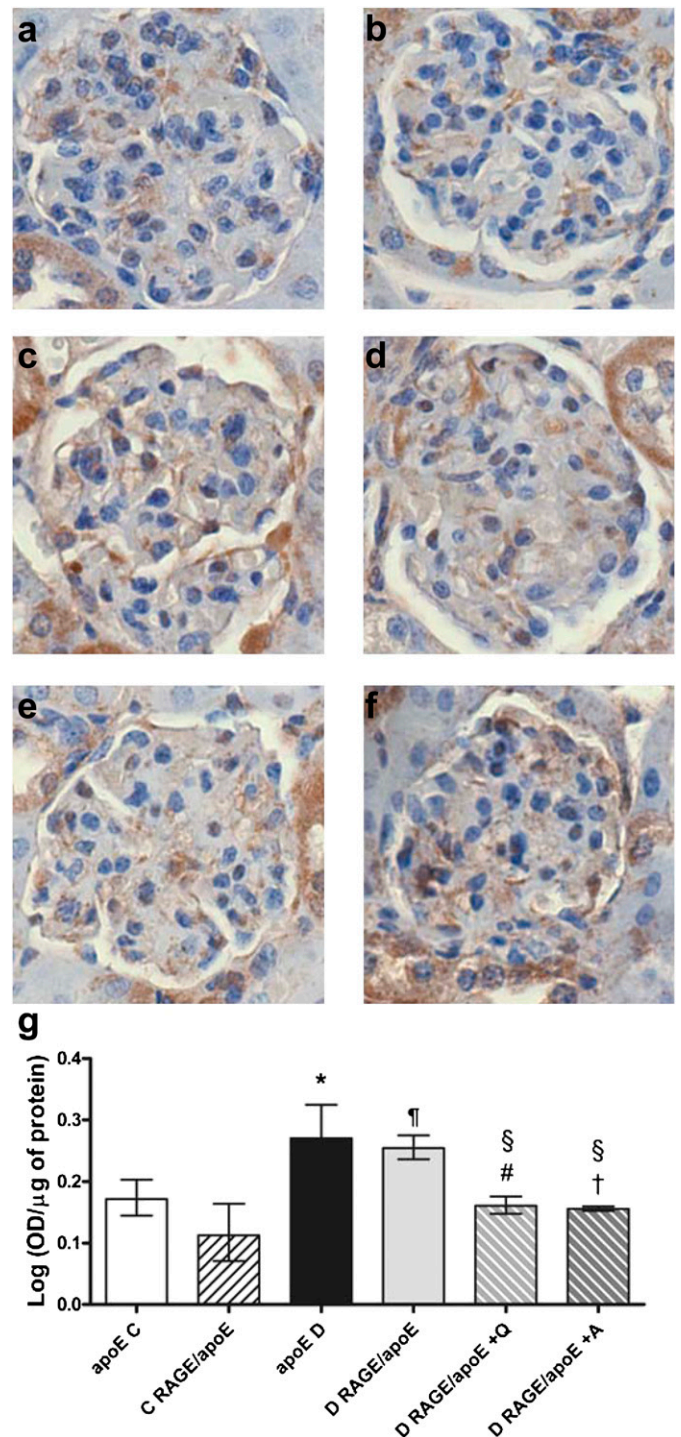


FIG. 6. Immunostaining for AGEs in nondiabetic control (C) and diabetic (D) *apoE* KO and RAGE *apoE* double-KO mice, with and without treatment. *ApoE* KO (a); RAGE *apoE* KO (b); diabetic *apoE* KO (c); diabetic RAGE *apoE* KO (d); diabetic RAGE *apoE* KO + alagebrium (A) (1 mg/kg/day) (e); diabetic RAGE *apoE* KO + quinapril (Q) (30 mg/kg/day) (f). Renal cortical AGE content by ELISA (g) using the same antibody as used for immunohistochemistry for  $n = 5-6$  per group. Data are presented as the geometric mean  $\pm$  tolerance factor.  $P < 0.05$  ( $n = 6-10$  per group). \* $P < 0.05$  vs. *apoE* KO. § $P < 0.05$  vs. diabetic *apoE* KO. ¶ $P < 0.05$  vs. RAGE *apoE* KO. # $P < 0.05$  diabetic RAGE *apoE* KO vs. diabetic RAGE *apoE* KO + quinapril. † $P < 0.05$  diabetic RAGE *apoE* KO vs. diabetic RAGE *apoE* KO + alagebrium. (A high-quality color representation of this figure is available in the online issue.)



## REFERENCES

1. Thomas MC. Advanced glycation end products. *Contrib Nephrol* 2011;170:66–74
2. Peppas M, Brem H, Cai W, et al. Prevention and reversal of diabetic nephropathy in db/db mice treated with alagebrium (ALT-711). *Am J Nephrol* 2006;26:430–436
3. Calcutt NA, Cooper ME, Kern TS, Schmidt AM. Therapies for hyperglycaemia-induced diabetic complications: from animal models to clinical trials. *Nat Rev Drug Discov* 2009;8:417–429
4. Lassila M, Seah KK, Allen TJ, et al. Accelerated nephropathy in diabetic apolipoprotein e-knockout mouse: role of advanced glycation end products. *J Am Soc Nephrol* 2004;15:2125–2138
5. Williams ME, Bolton WK, Khalifah RG, Degenhardt TP, Schotzinger RJ, McGill JB. Effects of pyridoxamine in combined phase 2 studies of patients with type 1 and type 2 diabetes and overt nephropathy. *Am J Nephrol* 2007;27:605–614
6. Babaei-Jadidi R, Karachalias N, Ahmed N, Battah S, Thornalley PJ. Prevention of incipient diabetic nephropathy by high-dose thiamine and benfotiamine. *Diabetes* 2003;52:2110–2120
7. Forbes JM, Thallas V, Thomas MC, et al. The breakdown of preexisting advanced glycation end products is associated with reduced renal fibrosis in experimental diabetes. *FASEB J* 2003;17:1762–1764
8. Vlassara H, Striker LJ, Teichberg S, Fuh H, Li YM, Steffes M. Advanced glycation end products induce glomerular sclerosis and albuminuria in normal rats. *Proc Natl Acad Sci USA* 1994;91:11704–11708
9. D'Agati V, Schmidt AM. RAGE and the pathogenesis of chronic kidney disease. *Nat Rev Nephrol* 2010;6:352–360
10. Sourris KC, Morley AL, Koitka A, et al. Receptor for AGEs (RAGE) blockade may exert its renoprotective effects in patients with diabetic nephropathy via induction of the angiotensin II type 2 (AT2) receptor. *Diabetologia* 2010;53:2442–2451
11. Reiniger N, Lau K, McCalla D, et al. Deletion of the receptor for advanced glycation end products reduces glomerulosclerosis and preserves renal function in the diabetic OVE26 mouse. *Diabetes* 2010;59:2043–2054
12. Tan AL, Sourris KC, Harcourt BE, et al. Disparate effects on renal and oxidative parameters following RAGE deletion, AGE accumulation inhibition, or dietary AGE control in experimental diabetic nephropathy. *Am J Physiol Renal Physiol* 2010;298:F763–F770
13. Yamamoto Y, Kato I, Doi T, et al. Development and prevention of advanced diabetic nephropathy in RAGE-overexpressing mice. *J Clin Invest* 2001;108:261–268
14. Wendt TM, Tanji N, Guo J, et al. RAGE drives the development of glomerulosclerosis and implicates podocyte activation in the pathogenesis of diabetic nephropathy. *Am J Pathol* 2003;162:1123–1137
15. Soro-Paavonen A, Watson AM, Li J, et al. Receptor for advanced glycation end products (RAGE) deficiency attenuates the development of atherosclerosis in diabetes. *Diabetes* 2008;57:2461–2469
16. Watson AM, Li J, Schumacher C, et al. The endothelin receptor antagonist avosentan ameliorates nephropathy and atherosclerosis in diabetic apolipoprotein E knockout mice. *Diabetologia* 2010;53:192–203
17. Krege JH, Hodgin JB, Hagaman JR, Smithies O. A noninvasive computerized tail-cuff system for measuring blood pressure in mice. *Hypertension* 1995;25:1111–1115
18. Allen TJ, Cooper ME, Lan HY. Use of genetic mouse models in the study of diabetic nephropathy. *Curr Diab Rep* 2004;4:435–440
19. Watson AM, Soro-Paavonen A, Sheehy K, et al. Delayed intervention with AGE inhibitors attenuates the progression of diabetes-accelerated atherosclerosis in diabetic apolipoprotein E knockout mice. *Diabetologia* 2011;54:681–689
20. Giunti S, Calkin AC, Forbes JM, et al. The pleiotropic actions of rosuvastatin confer renal benefits in the diabetic Apo-E knockout mouse. *Am J Physiol Renal Physiol* 2010;299:F528–F535
21. Miller AG, Tan G, Binger KJ, et al. Candesartan attenuates diabetic retinal vascular pathology by restoring glyoxalase-I function. *Diabetes* 2010;59:3208–3215
22. Candido R, Forbes JM, Thomas MC, et al. A breaker of advanced glycation end products attenuates diabetes-induced myocardial structural changes. *Circ Res* 2003;92:785–792
23. Forbes JM, Cooper ME, Thallas V, et al. Reduction of the accumulation of advanced glycation end products by ACE inhibition in experimental diabetic nephropathy. *Diabetes* 2002;51:3274–3282
24. Liliensiek B, Weigand MA, Bierhaus A, et al. Receptor for advanced glycation end products (RAGE) regulates sepsis but not the adaptive immune response. *J Clin Invest* 2004;113:1641–1650
25. Nasreddine N, Borde C, Gozlan J, Bélec L, Maréchal V, Hocini H. Advanced glycation end products inhibit both infection and transmission in trans of HIV-1 from monocyte-derived dendritic cells to autologous T cells. *J Immunol* 2011;186:5687–5695
26. Ziyadeh FN, Hoffman BB, Han DC, et al. Long-term prevention of renal insufficiency, excess matrix gene expression, and glomerular mesangial matrix expansion by treatment with monoclonal antitransforming growth factor-beta antibody in db/db diabetic mice. *Proc Natl Acad Sci USA* 2000;97:8015–8020
27. Zheng S, Noonan WT, Metreveli NS, et al. Development of late-stage diabetic nephropathy in OVE26 diabetic mice. *Diabetes* 2004;53:3248–3257
28. Myint KM, Yamamoto Y, Doi T, et al. RAGE control of diabetic nephropathy in a mouse model: effects of RAGE gene disruption and administration of low-molecular weight heparin. *Diabetes* 2006;55:2510–2522
29. Iacobini C, Amadio L, Oddi G, et al. Role of galectin-3 in diabetic nephropathy. *J Am Soc Nephrol* 2003;14(Suppl. 3):S264–S270
30. Lu C, He JC, Cai W, Liu H, Zhu L, Vlassara H. Advanced glycation end-product (AGE) receptor 1 is a negative regulator of the inflammatory response to AGE in mesangial cells. *Proc Natl Acad Sci USA* 2004;101:11767–11772
31. Singh R, Barden A, Mori T, Beilin L. Advanced glycation end-products: a review. *Diabetologia* 2001;44:129–146
32. Thomas MC, Forbes JM, Cooper ME. Advanced glycation end products and diabetic nephropathy. *Am J Ther* 2005;12:562–572
33. Tarsio JF, Wigness B, Rhode TD, Rupp WM, Buchwald H, Furcht LT. Nonenzymatic glycation of fibronectin and alterations in the molecular association of cell matrix and basement membrane components in diabetes mellitus. *Diabetes* 1985;34:477–484
34. Charonis AS, Tsilbary EC. Structural and functional changes of laminin and type IV collagen after nonenzymatic glycation. *Diabetes* 1992;41(Suppl. 2):49–51
35. Niwa T, Tsukushi S. 3-deoxyglucosone and AGEs in uremic complications: inactivation of glutathione peroxidase by 3-deoxyglucosone. *Kidney Int Suppl* 2001;78:S37–S41
36. Christ M, Bauersachs J, Liebetrau C, Heck M, Günther A, Wehling M. Glucose increases endothelial-dependent superoxide formation in coronary arteries by NAD(P)H oxidase activation: attenuation by the 3-hydroxy-3-methylglutaryl coenzyme A reductase inhibitor atorvastatin. *Diabetes* 2002;51:2648–2652
37. Loughlin DT, Artlett CM. Precursor of advanced glycation end products mediates ER-stress-induced caspase-3 activation of human dermal fibroblasts through NAD(P)H oxidase 4. *PLoS ONE* 2010;5:e11093
38. Sassy-Prigent C, Heudes D, Mandet C, et al. Early glomerular macrophage recruitment in streptozotocin-induced diabetic rats. *Diabetes* 2000;49:466–475
39. Chow FY, Nikolic-Paterson DJ, Ozols E, Atkins RC, Rollin BJ, Tesch GH. Monocyte chemoattractant protein-1 promotes the development of diabetic renal injury in streptozotocin-treated mice. *Kidney Int* 2006;69:73–80
40. Chow FY, Nikolic-Paterson DJ, Ozols E, Atkins RC, Tesch GH. Intercellular adhesion molecule-1 deficiency is protective against nephropathy in type 2 diabetic db/db mice. *J Am Soc Nephrol* 2005;16:1711–1722
41. Gu L, Hagiwara S, Fan Q, et al. Role of receptor for advanced glycation end-products and signalling events in advanced glycation end-product-induced monocyte chemoattractant protein-1 expression in differentiated mouse podocytes. *Nephrol Dial Transplant* 2006;21:299–313
42. Guo ZJ, Niu HX, Hou FF, et al. Advanced oxidation protein products activate vascular endothelial cells via a RAGE-mediated signaling pathway. *Antioxid Redox Signal* 2008;10:1699–1712
43. Forbes JM, Thorpe SR, Thallas-Bonke V, et al. Modulation of soluble receptor for advanced glycation end products by angiotensin-converting enzyme-1 inhibition in diabetic nephropathy. *J Am Soc Nephrol* 2005;16:2363–2372
44. Forbes JM, Yee LT, Thallas V, et al. Advanced glycation end product interventions reduce diabetes-accelerated atherosclerosis. *Diabetes* 2004;53:1813–1823
45. Davis BJ, Forbes JM, Thomas MC, et al. Superior renoprotective effects of combination therapy with ACE and AGE inhibition in the diabetic spontaneously hypertensive rat. *Diabetologia* 2004;47:89–97